A Dissected Ring Current Model for Assessing Magnetic Aromaticity: A General Approach for both Organic and Inorganic Rings

CINA FOROUTAN-NEJAD,[1] SHANT SHAHBAZIAN,[2] FERRAN FEIXAS,[3] PARVIZ RASHIDI-RANJBAR,[1] MIQUEL SOLÀ[3]
[1]*School of Chemistry, College of Science, University of Tehran, Tehran, Iran*
[2]*Faculty of Sciences, Department of Chemistry, Shahid Beheshti University, G.C., Evin, Tehran, Iran*
[3]*Institut de Química Computacional and Department de Química, Universitat de Girona, Campus de Montilivi, Girona 17071, Catalonia, Spain*

Received 24 January 2011; Revised 1 March 2011; Accepted 27 March 2011
DOI 10.1002/jcc.21824
Published online 19 May 2011 in Wiley Online Library (wileyonlinelibrary.com).

Abstract: A model based on classical electrodynamics is used to measure the strength of ring currents of different molecular orbitals, i.e., σ- and π-orbitals, and characteristics of ring current loops, i.e., ring current radii and height of current loops above/below the ring planes, among a number of organic as well as inorganic molecules. For the π-current, the present model represents an improvement of previous approaches to determine ring current intensity. It is proven that the present model is more precise than previous models as they could not explain presence of the minimum in the plot of $NICS_{\pi zz}$ versus distance close to the ring plane. Variations in the charge of molecules and the types of constituent atoms of each species affect the ring current radii of both σ- and π-current loops as well as the height of π-current loops above/below the ring plane. It is suggested that variation in the distribution of the one-electron density in different systems is the main source of differences of the ring current characteristics.

 J Comput Chem 32: 2422–2431, 2011

Key words: aromaticity; ring current model; magnetic shielding; electron density

Introduction

Aromaticity has been one of the most controversial issues in chemistry from the dawn of modern chemistry to date.[1] In recent years, many peculiar species have been marked as aromatic or antiaromatic[2] and various qualitative as well as quantitative methods were introduced for measuring the so-called aromaticity.[3] The comparison of outcomes of various methods and examination of strange molecules has aroused many arguments regarding the one dimensionality/multidimensionality of aromaticity,[4] e.g., energetic aromaticity, structural aromaticity, electronic aromaticity, and magnetic aromaticity. However, the true nature of aromaticity remains undetermined, and it is not clear to what extent the common aromaticity indices measure aromaticity solely; such issues have been well discussed in recent years.[5]

In the paradigm of *magnetic aromaticity*, it is assumed that the stronger the ring current intensity of a molecule, higher is the degree of its aromaticity. Among various indices that measure magnetic aromaticity the nucleus-independent chemical shift (NICS) is one of the most used.[6] NICS has been developed into many variants,[7] criticized from time to time, and has its opponents and proponents.[8] The magnitude of NICS partly reflects the intensity of ring currents, however, by relying on local information gathered from a single or a handful of points it is always plausible that certain features relevant to the intensity of ring currents may be lost.[9] The origin of this deficiency can be understood by constructing simplified models based on classical electrodynamics[10] or more precisely by comparing the results of NICS calculations and ring current analysis.[11]

In this contribution, previously proposed models of ring current based on classical electrodynamics are revised carefully. The reasons for the superiority of the present model to previously proposed models are discussed, and the validity of the most refined single point NICS methods, $NICS(0)_{\sigma zz}$ and $NICS(0)_{\pi zz}$, for a number of hydrocarbons, metallic, nonmetallic, and mixed clusters is examined. It is shown that in the context of the revised ring current model some discrepancies between magnetic paradigm of aromaticity and electronic aromaticity can be solved, and the results of different magnetic indicators of aromaticity are in line with each other. Also, it is demonstrated how the nature of atoms and the number of electrons influence the characteristics of electronic currents in terms of classical

Additional Supporting Information may be found in the online version of this article.

Correspondence to: Miquel Solà; e-mail: miquel.sola@udg.edu or Parviz Rashidi-Ranjbar; e-mail: ranjbar@khayam.ut.ac.ir

electrodynamics. Finally, the role of σ and π electrons in the magnetic aromaticity of double aromatic species are considered and compared with the π-aromaticity of well-known aromatic hydrocarbons in light of the proposed model.

Methods and Calculations

All structures, Figure S-1, were optimized at B3LYP[12]/6-311+G(d,p)[13] level by the Gaussian 98[14] suite of programs. The second derivatives of the energy were computed to ensure the local minima nature of species. Dissected (σ and π) NICS values were computed at the same computational level employing NBO 5.0,[15] as implemented in the Gaussian 98, by measuring the contributions of each canonical molecular orbital in total magnetic shielding, i.e., CMO-NICS.[16] The amount of electron density at different points of space and the iso-surfaces of electron density for different species were analyzed and depicted by the AIM2000 package.[17] The atomic volumes of "atoms in molecules" were computed by AIMAll suite of programs,[18] whereas the accuracy of calculations was guaranteed by keeping the basin integral of the Laplacian of the electron density in each atomic basin below 10^{-4} au.

It is well known that the source of unusual magnetic shieldings around the center of aromatic rings (as well as deshielding in the periphery of their rings) are the induced magnetic field originating from the induced electronic ring currents in the presence of an external magnetic field.[11] Ring current intensities for σ and π systems (I_σ and I_π) were calculated by fitting $NICS_{\sigma zz}$ ($NICS_{\pi zz}$) against the perpendicular distance from the center of ring plane using equations derived from classical electrodynamics and the Bio-Savart law. For this purpose, 50 $NICS_{\sigma zz}$ ($NICS_{\pi zz}$) values were computed in 0.1 Å intervals from non-weighted geometric center of each molecule up to 4.9 Å above the ring plane. Interestingly, the final result of the regression procedure, which shows correlation coefficients very close to unity, was independent from the initial guess of the parameters demonstrating the robustness of the model.

$$\sigma_\sigma = -\frac{\mu_0 I_\sigma}{2B_{ext}} \frac{R^2}{(R^2+z^2)^{3/2}} \tag{1}$$

$$\sigma_\pi = -\frac{\mu_0 I_\pi}{2B_{ext}} \left(\left(\frac{R^2}{(R^2+(z-r)^2)^{3/2}} \right) + \left(\frac{R^2}{(R^2+(z+r)^2)^{3/2}} \right) \right) \tag{2}$$

In eqs. (1) and (2), it is assumed that electronic currents are flowing in infinitely narrow superconductor circular wires. Although assuming a circular narrow wire is a simplification, this model provides valuable information as has been shown in several works.[10] In these equations I denotes the ring current intensity, μ_0 is the permeability of vacuum, B_{ext} is the external applied magnetic field, R is the current radius, and z is the variable which stands for the perpendicular distance from the current loop center whereas σ_σ and σ_π denote the magnetic shieldings of σ and π electrons at every point, respectively. In eq. (2), an additional parameter is included: r defines the distance of π current loop above and below the ring plane. This parameter has not been included in any of previously proposed classical ring current models, e.g., ARCS.[10b] The result of each regression for every molecule is a unique set of parameters namely, R, r, and I (assuming $-\frac{\mu_0}{2B_{ext}} = 1$ for simplicity) that emerged as described above, from a nonlinear fitting of $NICS_{\sigma zz}$ ($NICS_{\pi zz}$) values to eqs. (1) and (2). A detailed analysis of the distribution of π-electron density in a molecule shows that π-electron density is equal to zero on the ring plane of (planar) molecules, as the ring plane is the nodal plane of the π-system. The π-electron density increases gradually above or below the ring plane (nodal plane of the π-system) and after reaching a maximum decreases steeply, Figure 1. It is worth mentioning that electron density in the center (and above the center) of smaller rings is more than that of larger rings. This pattern is the result of the known exponential decay of charge density beyond the core region of free and bonded atoms;[19] this and the fact that the ring center as well as other points above and below the ring are farther than the nuclei in larger rings illuminate this observation namely the lower amount of electron density in the aforementioned points for larger rings.

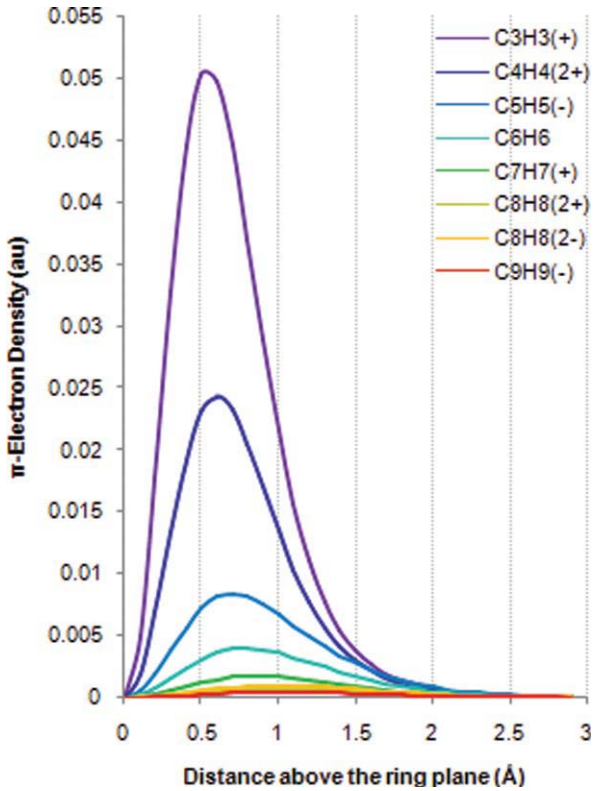

Figure 1. The plot of π-electron density versus distance above the geometrical ring center of eight aromatic hydrocarbons; π-electron density clearly is zero on the ring plane but increases by increasing the distance and then decreases again.

As in the ring plane $\rho_\pi = 0$, one may not find π-electronic currents in the ring plane of a *planar* molecule; this is also in line with current density analysis studies.[20a] Our primary investigations in this study demonstrates that without a model with *two* current loops [(like eq. (2)] the computed σ_π values deviate dramatically from $NICS_{\pi zz}$ values in distances near the ring plane.

Table 1. I_π (π-Ring Current Intensity)[a], R (Ring Current Radius), r (Height of Ring Current Loop Above and Below the Ring Plane) and Ring Radius in Å for the Three Groups of π-Aromatic Hydrocarbons. cc shows the correlation coefficient for the regression of eq. 2. $NICS(0)_{\pi zz}$ values in ppm are presented for comparison with current intensities.

	I_π[b]	R	r	cc	Ring radius	$NICS(0)_{\pi zz}$
$C_3H_3^+$	11.97	0.881	0.627	0.998650	0.787	−14.09
$C_4H_4^{2+}$	11.77	1.051	0.572	0.999916	0.989	−15.05
$C_5H_5^-$	34.56	1.468	0.672	0.999756	1.204	−34.98
C_6H_6	36.04	1.551	0.670	0.999954	1.395	−35.76
$C_7H_7^+$	36.85	1.701	0.674	0.999983	1.609	−34.72
$C_8H_8^{2+}$	37.24	1.892	0.679	0.999988	1.840	−32.75
$C_8H_8^{2-}$	59.34	2.059	0.692	0.999974	1.851	−48.94
$C_9H_9^-$	60.43	2.183	0.693	0.999992	2.050	−47.87

[a]For calculation of I values it is assumed that $-\mu_0/2B$ equals to 1 so I values are relative intensities and will change in different magnetic fields. However, variation in the relative intensities of currents will remain the same for different molecules in every arbitrarily chosen magnetic field.

[b]There are two π-current loops above and below the ring plane; the I_π values represent the intensity of each of these currents individually so the overall π-current intensity is twice the I_π values.

However, by increasing the distance from the ring plane, z, when r can be neglected compared with z, or when the ring radius or R are large compared with the r, eq. (1) can predict σ_π values relatively close to NICS values as it was also shown in case of ARCS methodology.[10b] On the other hand, one cannot guarantee that in distances far above the ring plane, e.g., more than 3 to 4 Å above the ring plane, *ab initio*/DFT derived shielding values are still reliable since usual Gaussian type basis sets are not designed for such long range purposes. Using eq. (2) for π currents improves the quality of shielding values, σ_π, dramatically, see Figures S-2 and S-8 for a pictorial comparison of the results of double-current versus single-current loop model, which demonstrates superiority of the former. Tables 1 to 3 present correlation coefficients between the calculated σ_π from regression procedure [from eq. (2)] and directly calculated $NICS_{\pi zz}$ values; it can be seen that the latter are perfectly reproduced. Remarkable trends are evident in these tables that are discussed in the next section. The σ_π values derived from eq. (2), i.e., two-current loop model, are superior to shielding values derived from the eq. (1), i.e., one-current loop model. Figures 2, S-2 and S-8 depict $NICS_{\pi zz}$ values versus (1) $NICS_{\pi zz}$ values, which is a reference straight line, (2) σ_π values derived from eq. (2) which are very close to $NICS_{\pi zz}$ values and (3) shielding values derived from fitting $NICS_{\pi zz}$ values into the eq. (1), i.e., π-current with one current loop; these figures prove superiority of double loop model.

Results and Discussions

Aromatic Hydrocarbons

Table 1 contains the final results of the regression analysis for the considered planar hydrocarbons. Among different hydrocarbons with various total charges (from +2 to −2) the current loop radius, R, is slightly larger than the ring radius (the latter is measured as the average distance of each nucleus from the geometrical center of the ring). Current loop radii, R values, obtained from eq. (2), are 12.0, 6.3, 21.9, 11.2, 5.7, 2.9, 11.3, and 6.5% larger than the ring radii for $C_3H_3^+$, $C_4H_4^{2+}$, $C_5H_5^-$, C_6H_6, $C_7H_7^+$, $C_8H_8^{2+}$, $C_8H_8^{2-}$, and $C_9H_9^-$ respectively. It is worth noting that the ring radii are defined as the distance between the ring center and the carbon nuclei of molecules. However, all current loop radii are smaller than the distance between the protons and ring center, so our model confirms that protons are in the deshielding zone of induced ring current as is expected from the known proton chemical shifts as well as the ring current model.[21b,c] This trend is in line with recent independent studies that also demonstrate that ring current radii are indeed larger than the ring radii for various hydrocarbons.[20] Both, the increase in ring size and total positive charge decrease the difference between the ring current loop radius and the ring radius. On the other hand, the variation of the total charge does not affect r values much; they are similar for species with the same number of π-electrons but when the number of π-electrons increases, the r values also increase gradually. This trend is in line with the shift of the maximum of ρ_π to larger distances from the ring center as is evident in Figure 1.

The relative intensities of π-ring currents, I_π, clearly demonstrate that the strength of electronic currents is proportional to the number of π-electrons; the I_π values in 10-π-electron species, cyclooctatetraene dianion and cyclononatetraenyl anion are about five times greater than that of 2π-electron molecules and 5/3 more than that of 6π-electron systems. Generally, it seems that I_π

Table 2. I_π (π-Ring Current Intensity)[a], R (Ring Current Radius), r (Height of Ring Current Loop Above and Below the Ring Plane), and Ring Radius in Å for Inorganic π-Aromatic Species. cc shows the correlation coefficient for the regression of eq. 2. $NICS(0)_{\pi zz}$ values in ppm are presented for comparison with current intensities.

	I_π[b]	R	r	cc	Ring radius	$NICS(0)_{\pi zz}$
P_5^-	32.62	1.984	0.937	0.999949	1.808	−24.18
S_5^{4+}	24.63	1.873	0.762	0.999993	1.805	−20.86
Se_5^{4+}	28.09	2.078	0.824	0.999992	2.030	−21.69
P_4S	27.23	1.975	0.891	0.999994	1.791	−20.85
$P_3S_2^+$	24.93	1.942	0.855	0.999999	1.780	−19.68
$P_2S_3^{2+}$	24.53	1.897	0.822	0.999996	1.780	−19.96
PS_4^{3+}	24.02	1.882	0.789	0.999997	1.783	−20.00
P_4Se	28.21	2.010	0.903	0.999991	1.837	−21.26
$P_3Se_2^+$	27.07	2.019	0.875	0.999997	1.868	−20.70
$P_2Se_3^{2+}$	28.07	2.008	0.853	0.999990	1.911	−21.75
PSe_4^{3+}	27.23	2.044	0.837	0.999994	1.964	−21.09

[a]For calculation of I values it is assumed that $-\mu_0/2B$ equals to 1 so I values are relative intensities and will change in different magnetic fields. However, variation in the relative intensities of currents will remain the same for different molecules in every arbitrarily chosen magnetic field.

[b]There are two π-current loops above and below the ring plane; the I_π values represent the intensity of each of these currents individually so the overall π-current intensity is twice the I_π values.

Table 3. I_π (π-ring current intensity)[a], R (ring current radius), r (height of ring current loop above and below the ring plane) and ring radius in Å for double aromatic species; cc shows the correlation coefficient for the regression of eq. 2. $NICS(0)_{\pi zz}$ and $NICS(0)_{\pi zz}{}^{rcp}$ values in ppm are presented for comparison with current intensities.

	I_π[b]	R	r	cc	Ring radius	$NICS(0)_{\pi zz}$	$NICS(0)_{\pi zz}{}^{rcp}$
Al_4^{2-}	13.15	2.144	1.395	0.996206	1.833	−6.91	−6.91
Si_4^{2+}	12.28	1.571	0.991	0.999331	1.633	−9.23	−9.23
Ga_4^{2-}	13.38	2.148	1.332	0.996400	1.815	−7.34	−7.34
Ge_4^{2+}	12.95	1.625	1.016	0.999404	1.740	−9.51	−9.51
Al_3Si^-	11.71	1.875	1.241	0.998661	1.752	−7.02	−6.66
Al_2Si_2	10.44	1.797	1.149	0.999516	1.709	−6.82	−6.01
$AlSi_3^+$	11.42	1.619	1.050	0.999225	1.653	−8.11	−6.68
Al_3Ga^{2-}	12.88	2.182	1.384	0.995341	1.835	−6.79	−6.78
$Al_2Ga_2^{2-}$	13.17	2.158	1.360	0.995921	1.822	−7.07	−7.06
$AlGa_3^{2-}$	13.26	2.128	1.342	0.996454	1.817	−7.24	−7.24
Al_3Ge^-	11.96	1.894	1.241	0.998714	1.770	−7.17	−6.78
Al_2Ge_2	11.15	1.816	1.148	0.999496	1.746	−7.28	−6.48
$AlGe_3^+$	12.29	1.651	1.062	0.999285	1.722	−8.65	−7.54
Ga_3Si^-	12.15	1.865	1.216	0.998816	1.743	−7.45	−7.16
Ga_2Si_2	10.70	1.769	1.138	0.999514	1.708	−7.07	−6.26
$GaSi_3^+$	11.30	1.630	1.055	0.999362	1.664	−8.02	−6.84
Ga_3Ge^-	12.40	1.890	1.220	0.998865	1.764	−7.58	−7.32
Ga_2Ge_2	11.33	1.803	1.142	0.999513	1.748	−7.45	−6.73
$GaGe_3^+$	12.11	1.668	1.066	0.999400	1.732	−8.50	−7.42
Si_3Ge^{2+}	12.41	1.578	0.998	0.999348	1.660	−9.28	−9.27
$Si_2Ge_2^{2+}$	12.47	1.597	1.006	0.999390	1.689	−9.25	−9.24
$SiGe_3^{2+}$	12.72	1.607	1.011	0.999395	1.714	−9.40	−9.39

[a]For calculation of I values it is assumed that $-\mu_0/2B$ equals to 1 so I values are relative intensities and will change in different magnetic fields. However, variation in the relative intensities of currents will remain the same for different molecules in every arbitrarily chosen magnetic field.

[b]There are two π-current loops above and below the ring plane; the I_π values represent the intensity of each of these currents individually so the overall π-current intensity is twice the I_π values.

values increase in molecules with the same number of π-electrons when the ring size increases. This trend is in line with results of our previous studies.[8e] It is worth noting that among different hydrocarbons, the 6π-electron hydrocarbons have the largest I_π values per electron. This should be noted that I_π values in Table 1 (Tables 2 and 3 in the manuscript) are reported for just one current loop of two loops in each π-aromatic species. Indeed the overall intensity of the π-currents is *twice* the reported values in Table 1 (Tables 2 and 3 in the manuscript).

It is of great interest to compare the ring current intensity values quantitatively with other magnetic indices like current density analysis and different $NICS(0)_{\pi zz}$ values. It is well known that the induced ring currents and the magnetic susceptibility are directly related to each other;[21] comparing the I_π with magnetic susceptibility of the π electrons of the studied species helps to evaluate the present model. The magnetic susceptibility of the π-systems for some of the molecules in the chosen set is reported in the literature.[22] The out-of-plane magnetic susceptibility of a given π-system is an appropriate criterion to be compared with the present results since, in the present model only the out-of-plane component of the shielding arising from the π-system is considered in eq. (2). It was shown that the out-of-plane magnetic susceptibilities of cyclopentadienyl anion and tropylium cation are 0.867 and 1.233 compared with that of benzene respectively, where the out-of-plane magnetic susceptibility of π-system in benzene was assumed to be unity. The order of these values is evidently in line with the order emerged from I_π values in Table 1, demonstrating the physical significance of the latter. Moreover, the trends in I_π values are quite similar to the results of electron density versus $NICS_{zz}$ scans[8e] for hydrocarbons even though these two methods are based on two different and seemingly unrelated methodologies. Comparing the maximum current density obtained from the current density analysis with the I_π values also confirms the validity of our model; Fowler and Soncini have reported the maximum current intensities for π-electrons of cyclopentadienyl anion (0.0702 a.u.), benzene (0.0784 a.u.) and tropylium cation (0.0814 a.u.) demonstrating that by increasing the ring size, current intensity also increases.[3k]

On the other hand, $NICS(0)_{\pi zz}$ values neither are in line with I_π nor with magnetizabilities, maximum current intensities of π systems or the electron density versus $NICS_{zz}$ scan plots.[8e] According to $NICS(0)_{\pi zz}$ the intensity of π ring currents for different species are only roughly related to the number of π electrons but in contrast to I_π values it is not linearly related to the number of π electrons. $NICS(0)_{\pi zz}$ values show that the intensities of ring currents per electron decrease dramatically from 2π-electron species to 6π-electron systems and then 10π-electron molecules while this trend is more constant for I_π values.

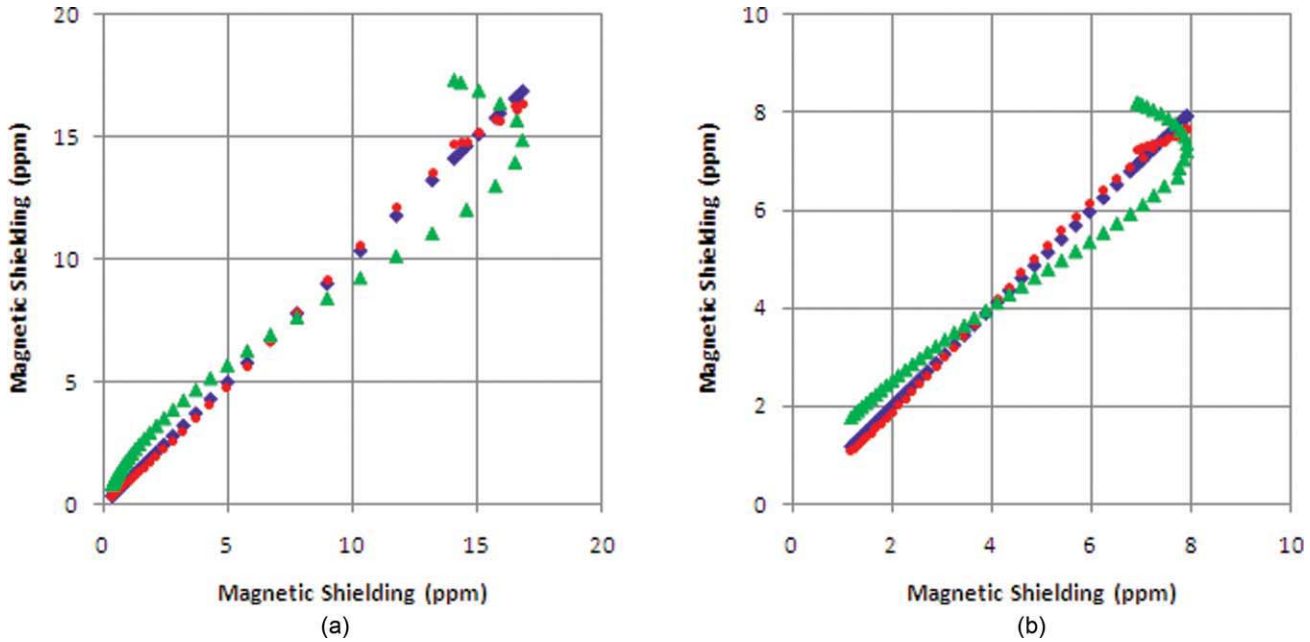

Figure 2. $NICS_{\pi zz}$ values versus (1) $NICS_{\pi zz}$ values, which is a straight reference line (blue rectangular), (2) σ_π values derived from eq. (2) which are very close to $NICS_{\pi zz}$ values (red circles) and (3) shielding values derived from fitting $NICS_{\pi zz}$ values into the eq. (1), i.e., π-current with one current loop (green triangles) for (a) cyclopropenyl cation and (b) Al_4^{2-}; this figure proves superiority of double loop model as points of series 1 and 2 almost coincide with each other while points of series 3 move around the straight line.

Although, single point $NICS_{\pi zz}$ values fail to determine the current intensity, they are yet useful for determining the current intensity if one employs eq. (2). As mentioned above, the results of the double-current loop model based on $NICS_{\pi zz}$ scan are very close to the results of current density analysis.

Inorganic π-Aromatic Species

To test the validity of the model beyond the domain of planar hydrocarbons a set of planar inorganic π-aromatic molecules are studied. This set includes 6π-electron $P_{5-n}S_n^{(n-1)}$ and $P_{5-n}Se_n^{(n-1)}$ species (n = 0–5) in which, unlike the hydrocarbons studied before, both molecular charge and atom types are varied. As is evident from the correlation coefficients in Table 2, the regression procedure is completely successful and the model fits ideally to the NICS data. The σ-framework of these molecules is not magnetically aromatic. This is in line with MCI data reported in a recent study.[23]

Among $P_{5-n}S_n^{(n-1)}$ and $P_{5-n}Se_n^{(n-1)}$ clusters the R values change by varying the total charge of molecules as it was observed for hydrocarbons. Ring current loops radii are again larger than the ring radii of each molecule but the relative size of R gradually decreases among $P_{5-n}S_n^{(n-1)}$ clusters by increasing the number of sulfur atoms (9.7, 10.3, 9.1, 6.6, 5.5, 3.8%) and similarly among $P_{5-n}Se_n^{(n-1)}$ species by increasing the number of selenium atoms (9.7, 9.4, 8.1, 5.1, 4.1, 2.4%). Among $P_{5-n}S_n^{(n-1)}$ and $P_{5-n}Se_n^{(n-1)}$ species, the r values decrease with the increase of the total positive charge and the number of chalcogen atoms, however, these are always larger than the r values of hydrocarbons. The latter trend seems to be legitimate since the size of P, S, and Se atoms are larger than that of carbon atom. Furthermore, the r value for selenium containing cluster is greater than their sulfur containing counterparts; this can be explained if one considers the role of *4p* orbitals in selenium and *3p* orbitals in sulfur in magnetic aromaticity. The I_π value for P_5^- in both sets is the largest while all the 6π-electron members of these sets have smaller currents than the 6π-electron hydrocarbons. Although $NICS(0)_{\pi zz}$ also predicts a larger current intensity for P_5^- than other members of these sets, a fine correlation between $NICS(0)_{\pi zz}$ and I_π values is not observed among other members. Let us mention here that $NICS(0)_{\pi zz}$ values of Table 2 have been computed at the non-weighted geometrical center of the different rings. The values of $NICS(0)_{\pi zz}^{rcp}$ obtained at the ring critical point (vide infra) are practically the same, the differences between $NICS(0)_{\pi zz}$ and $NICS(0)_{\pi zz}^{rcp}$ being never larger than few hundredths of a ppm.

Double Aromatic Species

The legitimacy of the model for a number of double aromatic (σ and π) molecules, which are composed of twenty two four-membered clusters of Al, Si, Ga, and Ge is studied heedfully. The obtained results are gathered in Tables 3 and 4. It is worth noting that for these systems $NICS(0)_{\sigma zz}$ and consequently I_σ values are obtained by summing the contributions of six σ-type valence molecular orbitals for each molecule. Studying the out-of-plane component of NICS demonstrates that six σ-orbitals contribute almost equally to the magnetic shielding. These sets were

Table 4. I_σ (σ-Ring Current Intensity)[a], R (Ring Current Radius) and Ring Radius in Å; $NICS(0)_{\sigma zz}$ and $NICS(0)_{\sigma zz}^{rcp}$ in ppm for σ-Aromatic Species. cc shows the correlation coefficient for the regression of eq. 1.

	I_σ	R	cc	Ring radius	$NICS(0)_{\sigma zz}$	$NICS(0)_{\sigma zz}^{rcp}$
Al_4^{2-}	141.77	2.359	0.999531	1.833	−60.68	−60.68
Si_4^{2+}	130.13	1.863	0.999855	1.633	−70.29	−70.29
Ga_4^{2-}	148.99	2.320	0.999786	1.815	−64.59	−64.59
Ge_4^{2+}	133.53	1.996	0.999994	1.740	−66.09	−66.09
Al_3Si^-	128.27	2.170	0.999558	1.752	−59.70	−57.81
Al_2Si_2	122.35	2.047	0.999645	1.709	−60.33	−57.38
$AlSi_3^+$	125.19	1.912	0.999735	1.653	−66.04	−61.92
Al_3Ga^{2-}	141.66	2.357	0.999636	1.835	−60.57	−60.52
$Al_2Ga_2^{2-}$	142.80	2.355	0.999715	1.822	−61.01	−60.97
$AlGa_3^{2-}$	143.24	2.348	0.999778	1.817	−61.32	−61.30
Al_3Ge^-	131.74	2.204	0.999692	1.770	−60.27	−58.71
Al_2Ge_2	129.08	2.099	0.999874	1.746	−61.81	−59.85
$AlGe_3^+$	130.88	1.993	0.999877	1.722	−65.87	−64.30
Ga_3Si^-	131.26	2.193	0.999894	1.743	−60.11	−59.07
Ga_2Si_2	120.42	2.067	0.999859	1.708	−58.60	−55.63
$GaSi_3^+$	122.08	1.935	0.999809	1.664	−63.54	−59.79
Ga_3Ge^-	134.51	2.215	0.999932	1.764	−60.92	−60.27
Ga_2Ge_2	127.63	2.117	0.999964	1.748	−60.42	−58.66
$GaGe_3^+$	129.31	2.024	0.999971	1.732	−64.02	−62.30
Si_3Ge^{2+}	128.95	1.889	0.999908	1.660	−68.58	−68.55
$Si_2Ge_2^{2+}$	127.58	1.918	0.999942	1.689	−66.74	−66.70
$SiGe_3^{2+}$	130.79	1.960	0.999981	1.714	−66.83	−66.80

[a]For calculation of I values it is assumed that $-\mu_0/2B$ equals to 1 so I values are relative intensities and will change in different magnetic fields. However, variation in the relative intensities of currents will remain the same for different molecules in every arbitrarily chosen magnetic field.

recently studied by Feixas et al. and general trends in their relative aromaticities based on electronic multicenter indices (MCI) were clearly identified.[23]

In each molecule of this set, two factors are changing: total charge and atom type; two factors that had a significant effect on the magnitude and characteristics of the electronic ring currents of π-aromatic species. However, relative changes in the π-current loop radii of π-currents among double aromatic species are much more significant compared with the π-aromatic inorganic and hydrocarbon systems. For negatively charged and neutral species, the current loop radii are larger than the molecular ring radii but for positively charged species the π-current loop radii are smaller than the ring radii. The height of π-current loops above and below the ring plane, r, is larger for metallic species and decreases by increasing the total positive charge of the cluster.

The σ-current loop radii vary among these species like the π-current loop radii as they are larger for metallic clusters. Furthermore, the σ-current loop radii for all double aromatic species are larger than their ring radii. Although, the current density maps of most of these systems have not been studied yet, a careful study on σ- and π-current density maps of Al_4^{2-} demonstrates that both σ- and π-current loops radii are indeed larger than the ring radius.[24]

Profiles of electron density versus distance for four pure double aromatic systems (Al_4^{2-}, Si_4^{2+}, Ga_4^{2-}, and Ge_4^{2+}) are depicted in Figure 3. It is seen that for metallic clusters where the current loop radius is large and far above the ring plane, the distribution of electron density is loose. On the other hand, for non-metallic species, where current loop radii of both σ- and π-systems are smaller than their metallic counterparts the distribution of electron density is much more compact. It seems that looseness/tightness of electron density distribution is qualitatively in line with the geometrical characteristics of current loops for metallic/non-metallic systems.

The relationship between geometrical characteristics of current loops and electron density distribution can be examined also by a more quantitative approach. Figure 4 depicts plots of R for σ-currents and $(R^2 + r^2)^{1/2}$ for π-currents versus sum of atomic volumes obtained from the Quantum Theory of Atoms in Molecules (QTAIM).[25] Atomic volumes reflect looseness/tightness of the contribution of electron density in four-membered ring clusters and are well correlated with current loop geometrical characteristics.

This shows that the distribution of electron density indeed affect the size and height of *effective* electronic current loops. The same relationship is not observed for hydrocarbons and inorganic π-aromatic compounds; for a discussion regarding possible reasons of this observation see SI.

I_σ and I_π values (Tables 3 and 4) follow the expected trends of relative aromaticity; ring current intensities of symmetric M_4 clusters is always greater than M_3N species, a result that is consistent with the recently computed MCI values[23] and is anticipated from geometrical criterion of aromaticity. Based on I_σ and I_π values, M_2N_2 species usually have the weakest

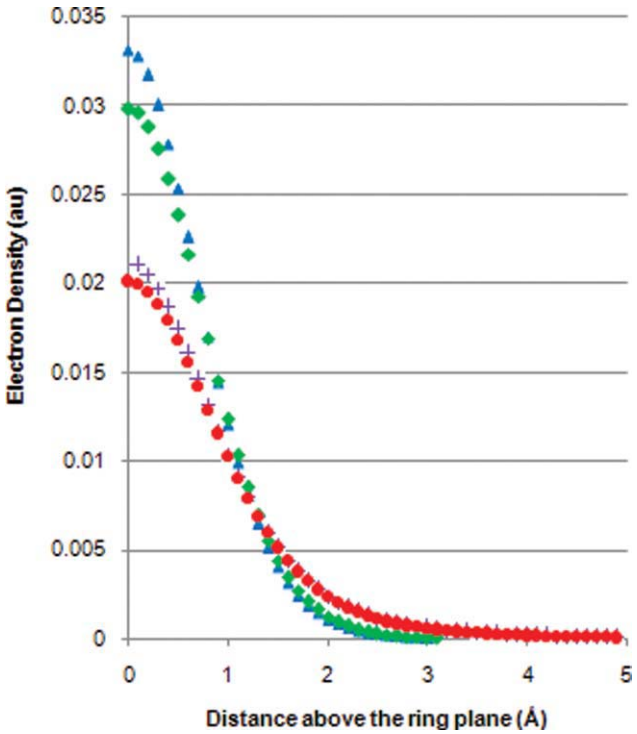

Figure 3. The plot of electron density versus distance for Al_4^{2-} (violet crosses), Ga_4^{2-} (red circles), Si_4^{2+} (blue triangles) and Ge_4^{2+} (green squares); electron density values are depicted to 5×10^{-5} threshold. The electron densities of Al_4^{2-} and Ga_4^{2-} is less than that of Si_4^{2+} and Ge_4^{2+} near the ring plane but electron density of Si_4^{2+} and Ge_4^{2+} drops below that of Al_4^{2-} and Ga_4^{2-} about 1 Å above the ring plane.

σ- and π-ring currents. However, in case of $Al_{4-n}Ga_n^{2-}$ species, Al_3Ga^{2-} has weakest σ- and π-electronic currents. Similarly among $Si_{4-n}Ge_n^{2+}$ clusters Si_3Ge^{2+} has the weakest π-current. According to I_π values among $Al_{4-n}Ga_n^{2-}$ and $Si_{4-n}Ge_n^{2+}$ clusters molecules with two or more number of Ga or Ge have stronger ring currents than Al_4^{2-} and Si_4^{2+} respectively. The same is true for I_σ in $Al_{4-n}Ga_n^{2-}$ systems. However, as is expected[23] within these two groups variation of ring current intensity is much smaller than the other molecules since both atoms of the $Al_{4-n}Ga_n^{2-}$ and $Si_{4-n}Ge_n^{2+}$ series come from the same group of the periodic table.

It is interesting to determine which species among Al_4^{2-}, Si_4^{2+}, Ga_4^{2-}, and Ge_4^{2+} has the strongest ring currents. According to I_σ and I_π values the order of strength of ring currents (both σ- and π-currents) for these species is as the following: $Ga_4^{2-} > Al_4^{2-} > Ge_4^{2+} > Si_4^{2+}$, it is interesting to note that a complex containing Ga_4^{2-}, the most aromatic species according to ring current strength is known and studied in bulk[26] but complexes of other species, to the best of our knowledge, are not yet known in bulk. Previous studies by ARCS methodology suggests that ring current intensity of Al_4^{2-} is somewhat stronger than Ga_4^{2-} and ring current radii of these species are smaller than their ring radii;[27] these results are in contrast to our computed intensities and the distribution of ring current vectors obtained from current density analysis.[20a,24]

A major question regarding double aromatic species is the relative contributions of σ- and π-electrons in magnetic aromaticity. This has been studied by means of different tools for Al_4^{2-} in particular.[23,24,28] A precise study based on current density analysis and out-of-plane dissected NICS suggest that σ-electronic currents are more intense than their π counterparts.[24] On the other hand, MCI and a number of other tools suggest that the role of π-aromaticity is more prominent than σ-aromaticity.[23,29] Since there is a direct relationship between the number of electrons and the intensity of induced magnetic field in an aromatic species, magnetic indices are influenced by the number of electrons. A recent study based on current density analysis shows that the intensity of π-currents per electron is more than that of σ-currents. Moreover, the overall intensity of σ-currents is almost six times greater than the intensity of π-currents.[20a] Comparing values of $NICS(0)_{\sigma zz}$ per electron with $NICS(0)_{\pi zz}$ per electron suggests that σ-framework with 12 valence electrons is more aromatic than π ($NICS(0)_{\sigma zz}$/e = −5.06 and

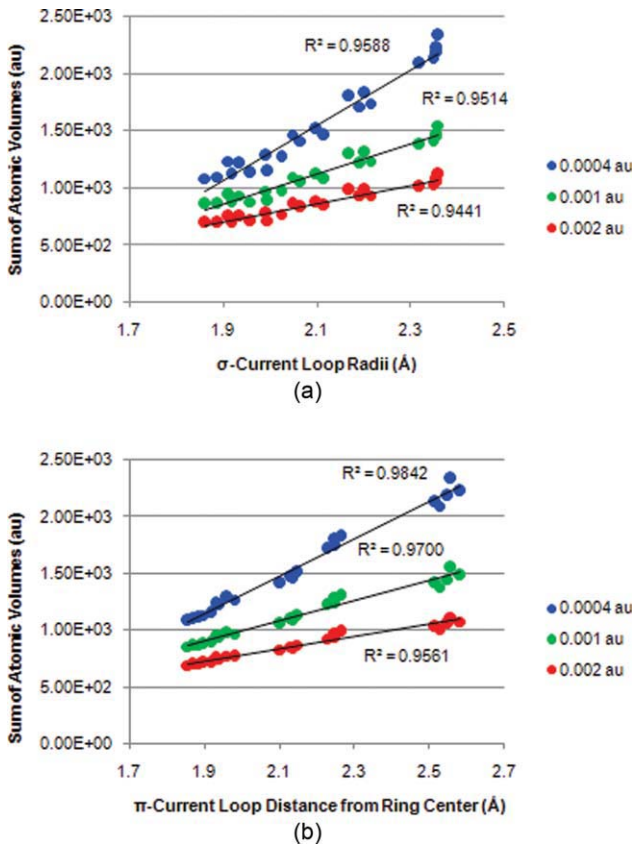

Figure 4. The plots of the sum of atomic volumes bound by three different iso-electronic surfaces (0.0004 au, 0.001 au, and 0.002 au) versus dimensions of electronic current loops in four-membered σ- and π-double aromatic species; better correlations are observed considering iso-electronic surfaces with lower isodensity values, maybe as a result of smoothing the molecular shape in lower electron density iso-electronic surfaces.

$NICS(0)_{\pi zz}/e = -3.45$ ppm). This result is neither in line with MCI results nor with current density analysis or the fact that π-electrons are less attracted by the positive charge of nuclei and hence are more amenable to produce an electronic current compared to σ-electrons. In contrast to single point NICS values, the strength of electronic currents per electron suggests that π-currents ($I_\pi/e = 13.15$) are slightly stronger than σ ones ($I_\sigma/e = 11.81$); this is in a complete agreement with current density analysis results.[20a] However, total magnetic contributions of six filled valence σ-orbitals of Al_4^{2-} is certainly more than its single π orbital as current density analysis suggests.[20a,24] It should be again emphasized that I_π values in Tables denote the current intensity for just one current loop of two current loops in each π-system. The same is true for the rest of four-membered ring clusters as their relative π-aromaticity is more than their σ-aromaticity. It is also worth noting that current density analysis demonstrates that the relative π-current intensity of benzene is almost three times more than that of Al_4^{2-}.[20a] I_π values in Tables 1 and 3 show exactly the same trend as current density analysis.

Although the $NICS(0)_{\sigma zz}$ and $NICS(0)_{\pi zz}$ are the most refined NICS variants (as they measure pure contributions of σ- or π-electrons whereas choosing the out-of-plane component of NICS guarantees that *in-plane ring currents* are being measured exclusively) studying the $NICS(0)_{\sigma zz}$ and $NICS(0)_{\pi zz}$ values in Tables 3 and 4 for different species show that these NICS variants do not obey the expected trends in the strength of electronic currents. According to $NICS(0)_{\sigma zz}$ and $NICS(0)_{\pi zz}$ values, Si_4^{2+} and Ge_4^{2+} have the strongest σ- and π-electronic currents among all double aromatic species, respectively. Surprisingly, NICS values suggest that replacing Al or Ga atoms with more electronegative Si and Ge atoms not only does not reduce the strength of ring currents as one expects, but also augment them. Particularly, $NICS(0)_{\pi zz}$ suffers from such flaws more than $NICS(0)_{\sigma zz}$. This flaw is also expected based on our model since the characteristics of π-electronic currents (the current loop radii and the height of current loops above or below the ring plane) vary more than those of σ-electronic currents. For instance, $NICS(0)_{\pi zz}$ values suggest that replacing Al atoms in Al_4^{2-} by any other atoms increases the strength of electronic ring current (there are only two exceptions, Al_2Si_2 and Al_3Ga^{2-}, according to NICS criterion that their $NICS(0)_{\pi zz}$ values are less negative than the Al_4^{2-}). Indeed, variations in the coordinates of current loops (R and z) seriously affect NICS values so $NICS(0)_{\sigma zz}$ and $NICS(0)_{\pi zz}$ cannot verify the correct order of ring current intensity. Alternatively, $NICS(0)_{\sigma zz}$ and $NICS(0)_{\pi zz}$ values can be computed at the ring critical point (rcp), i.e., the point of lowest electron density in the ring plane, instead of the geometrical ring center[30] in order to minimize the influence of electron density on the magnetic shielding.[8e] As can be seen from Tables 3 and 4, $NICS(0)^{rcp}_{\pi zz}$ improves the expected trends for most of molecules in the series analyzed, thus, the results are more in line with I_π and MCI calculations. The major flaw of the $NICS(0)^{rcp}_{\pi zz}$ (as of $NICS(0)_{\pi zz}$) is its inconsistency with the trend of I_π values of Al_4^{2-}, Si_4^{2+}, Ga_4^{2-}, and Ge_4^{2+} species where the ring current radii change dramatically.

$NICS(0)^{rcp}_{\sigma zz}$ performs better compared with its counterpart at the geometric center; particularly, among $Ga_{4-n}Si_n^{n-2}$ and $Ga_{4-n}Ge_n^{n-2}$ clusters it performs quite well. However, $NICS(0)^{rcp}_{\sigma zz}$ is not completely in line with I_σ for all species. This strong dependence on the chosen point of the space, where $NICS(0)_{\sigma zz}$ and $NICS(0)_{\pi zz}$ are calculated, was also observed by Feixas et al. for NICS(0), NICS(1), $NICS(0)_\sigma$, and $NICS(0)_\pi$.[23]

Concluding Remarks

Ring current intensities for a diverse set of molecules are estimated by a simple model from classical electrodynamics. Such models have been used for estimation of ring current intensity in terms of ARCS methodology before.[10b] In this contribution, the ARCS methodology is carefully revised by (1) employing dissected NICS values, e.g., contributions of σ and π frameworks are studied separately, (2) the out-of-plane component of shielding is used instead of isotropic shielding in order to eliminate the influence of electronic currents other than the ring current (3) for measuring the π-current intensity a double-loop model is used. Employing a double-loop model improves estimated shielding values, σ_π, both qualitatively and quantitatively compared with a single-loop model. By a single-loop model the minimum in the plot of $NICS_{\pi zz}$ values versus distance cannot be produced while the double-loop model is reasonably successful in this task, see Figure S-8.

It is shown that $NICS_{\sigma zz}$ and $NICS_{\pi zz}$ values are reproduced from basic equations of electrodynamics while a parameter of this eq., I, represents the strength of electronic currents. In the considered cases, the results of this model are consistent with chemical intuition, current density analysis data[3k,20,22] and MCI results[23] while single point NICS values are not so clearly in line with chemical intuition, MCI values and other considered magnetic indices. Interestingly, the performance of $NICS_{\sigma zz}$ and $NICS_{\pi zz}$ can be improved by calculating NICS values at the ring critical point instead of the geometrical ring center.

The geometrical characteristics of σ- and π-current loops in classical view vary by substituting the atoms of a molecule; among four-membered ring species a reasonable correlation is found between the sum of atomic volumes and both the σ- and π-current loop radii. Substituting the atoms of a molecule by more electronegative atoms triggers contraction of the electron distribution and consequently the decrease of the electronic current loop radii and atomic volumes. It was shown that in all species the current loop radius depends on the total charge of molecules while the height of π-current loops above and below the ring plane is not sensitive to the total charge (as it is evident in the case of hydrocarbons). On the other hand, atom type variations (and consequently the size, electronegativity and distribution of electron density) affect the height of π-current loops above/below the ring plane.

Furthermore, our model is in line with MCI and precise current density analysis results indicating that in Al_4^{2-} and related species the *relative* contribution of a π-electron in magnetic aromaticity is more than that of a σ-electron.

Difference between the characteristics of current loops in different species is the main source of NICS failure in determining the electronic current intensity and NICS calculations among species with different atom types is not a safe root for

measuring the ring current intensities. NICS variants are useful probes for qualitative purposes *if and only if* the out-of-plane component of magnetic shielding is used, e.g., $NICS(x)_{zz}$, $NICS(x)_{\sigma zz}$, and $NICS(x)_{\pi zz}$.

Comparing aromaticity orders based on this study with results obtained from a previous study[23] demonstrates that there are some differences between magnetic indexes and electron sharing indexes of aromaticity. These differences usually are interpreted in terms of multidimensionality of aromaticity.[4] However, this fact may also be seen from a different point of view as magnetic properties are *response* properties, whereas energetic, structural and electronic properties are ground state properties. Indeed, several factors, e.g., HOMO-LUMO gaps, affect magnetic properties that are not influential on ground state properties.

References

1. (a) Breslow, R. Acc Chem Res 1973, 6, 393; (b) Minkin, V. I.; Glukhovtsev, M. N.; Simkin, B. Y. Aromaticity and Antiaromaticity; Wiley: New York, 1994; (c) Schleyer, P. v. R.; Jiao, H. Pure Appl Chem 1996, 68, 209; (d) Lloyd, D. J Chem Inf Comput Sci 1996, 36, 442; (e) Krygowski, T. M.; Cyranski, M. K.; Czarnocki, Z.; Hafelinger, G.; Katritzky, A. R. Tetrahedron 2000, 56, 1783; (f) Schleyer, P. v. R., Guest Ed. Special Issue on Aromaticity. Chem Rev 2001, 101(5); (g) Schleyer, P. v. R., Guest Ed. Special Issue on Aromaticity. Chem Rev 2005, 105(10); 1(h) Stanger, A. Chem Commun 2009, 1939.
2. (a) Alvarado-Soto, L.; Ramírez-Tagle, R.; Arratia-Pérez, R. J Phys Chem A 2009, 113, 1671; (b) Alvarado-Soto, L.; Ramírez-Tagle, R.; Arratia-Pérez, R. Chem Phys Lett 2008, 467, 94; (c) Lee, V. Y.; Sekiguchi, A. Angew Chem Int Ed Engl 2007, 46, 6596; (d) Tsipis, A. C.; Kefalidis, C. E.; Tsipis, C. A. J Am Chem Soc 2008, 130, 9144; (e) Holtzl, T.; Nguyen, M. T.; Veszpremi, T. Phys Chem Chem Phys 2009, 12, 556; (f) Yu, H. -L.; Sang, R. -L.; Wu, Y. -Y. J Phys Chem A 2009, 113, 3382; (g) Huang, W.; Sergeeva, A.; Zhai, H-J.; Averkiev, B. B.; Wang, L-S., Boldyrev, A. I. Nature Chem 2010, 2, 202; (h) Bean, D. E.; Fowler, P. W. J Phys Chem A 2009, 113, 15569; (i) Tsipis, A. C.; Depastas, I. G.; Karagiannis, E. E.; Tsipis, C. A. J Comput Chem 2010, 31, 431; (j) Tsipis, A. C. Phys Chem Chem Phys 2009, 11, 8244; (k) Xu, Q.; Jiang, L.; Tsumori, N. Angew Chem Int Ed Engl 2005, 44, 4338; (l) Foroutan-Nejad, C.; Shahbazian, S.; Rashidi-Ranjbar, P. Phys Chem Chem Phys 2011, 13, 4576.
3. (a) Aihara, J. -I. J Phys Org Chem 2008, 21, 79; (b) Noorizadeh, S.; Dardab, M. Chem Phys Lett 2010, 493, 376; (c) Giambiagi, M.; de Giambiagi, M. S.; dos Santos, C. D.; de Figueiredo, A. P. Phys Chem Chem Phys 2000, 2, 3381; (d) Bultinck, P.; Ponec, R.; Van Damme, S. J Phys Org Chem 2005, 18, 706; (e) Bultinck, P.; Rafat, M.; Ponec, R.; van Gheluwe, B.; Carbó-Dorca, R.; Popelier, P. J Phys Chem A 2006, 110, 7642; (f) Fernández, I.; Frenking, G. Faraday Discuss 2007, 135, 403; (g) Mandado, M.; Gonzalez, M. J.; Mosquera, R. A. J Comput Chem 2006, 28, 127; (h) Matito, E.; Duran, M.; Solà M. J Chem Phys 2005, 122, 014109. Erratum: J Chem Phys 2006, 125, 059901; (i) Perez-Juste, I.; Mandado, M.; Carballeira, L. Chem Phys Lett 2010, 491, 224; (j) Koleva, G.; Galabov, B.; Wu, J. I-C., Schaefer, H. F.; Schleyer, P. v. R. J Am Chem Soc 2009, 131, 14722; (k) Fowler, P. W.; Soncini, A. Chem Phys Lett 2004, 383, 507; (l) Poater, J.; Fradera, X.; Duran, M.; Solà, M. Chem Eur J 2003, 9, 1113.
4. (a) Katritzky, A. R.; Barczynski, P.; Musumarra, G.; Pisano, D.; Szafran, M. J Am Chem Soc 1989, 111, 7; (b) Cyrański, M. K.; Krygowski, T. M.; Katritzky, A. R.; Schleyer, P. v. R. J Org Chem 2002, 67, 1333; (c) Jug, K.; Köster, A. M. J Phys Org Chem 1991, 4, 163.
5. Lazzeretti, P. Phys Chem Chem Phys 2004, 6, 217.
6. Schleyer, P. v. R.; Maerker, C.; Dransfeld, A.; Jiao, H.; Hommes, N. J. R. v. E. J Am Chem Soc 1996, 118, 6317.
7. Chen, Z.; Wannere, C. S.; Corminboeuf, C.; Puchta, R. Schleyer, P. v. R. Chem Rev 2005, 105, 3842.
8. (a) Wiberg, K. Chem Rev 2001, 101, 1317; (b) Stanger, A. J Org Chem 2006, 71, 883; (c) Jiménez-Halla, J. O. C.; Matito, E.; Robles, J.; Solà, M. J Organomet Chem 2006, 691, 4359; (d) Sergeeva, A. P.; Boldyrev, A. I. Comment Inorg Chem 2010, 31, 2; (e) Foroutan-Nejad, C.; Shahbazian, S.; Rashidi-Ranjbar, P. Phys Chem Chem Phys 2010, 12, 12630; (f) Stanger, A. Chem Eur J 2006, 12, 2745.
9. Carion, R.; Liegeois, V.; Champagne, B.; Bonifazi, D.; Pelloni, S.; Lazzeretti, P. J Phys Chem Lett 2010, 1, 1563.
10. (a) Buhl, M. Chem Eur J 1998, 4, 734; (b) Juselius, J.; Sundholm, D. Phys Chem Chem Phys 1999, 1, 3429; (c) Morao, I.; Cossío, F. P. J Org Chem 1999, 64, 1868.
11. (a) Lazzeretti, P. Progress in Nuclear Magnetic Resonance Spectroscopy, Elsevier: New York, 2000, 36, 1; (b) Mitchell, R. H. Chem Rev 2001, 101, 1301; (c) Gomes, J. A. N. F.; Mallion, R. B. Chem Rev 2001, 101, 1349; (d) Steiner, E.; Fowler, P. W. Chem Commun 2001, 2220; (e) Poater, J.; Solà, M.; Viglione, R. G.; Zanasi, R. J Org Chem 2004, 69, 7537; (f) Fias, S.; Van Damme, S.; Bultinck, P. J Comput Chem 2010, 31, 2286. (g) Osuna, S.; Poater, J.; Bofill, J. M.; Alemany, P.; Solà, M. Chem Phys Lett 2006, 428, 191.
12. (a) Becke, A. D. J Chem Phys 1993, 98, 5648; (b) Becke, A. D. Phys Rev A 1988, 38, 3098; (c) Lee, C.; Yang, W.; Parr R. G. Phys Rev B 1988, 37, 785; (d) Stephens, P. J.; Devlin, F. J.; Chabalowski, C. F.; Frisch, M. J. J Phys Chem 1994, 98, 11623.
13. (a) McLean, A. D.; Chandler, G. S. J Chem Phys 1980, 72, 5639; (b) Krishnan, R.; Binkley, J. S.; Seeger, R.; Pople, J. A. J Chem Phys 1980, 72, 650.
14. Frisch, M. J.; Trucks, G. W.; Schlegel, H. B.; Scuseria, G. E.; Robb, M. A.; Cheeseman, J. R.; Zakrzewski, V. G.; Montgomery, J. A., Jr.; Stratmann, R. E.; Burant, J. C.; Dapprich, S.; Millam, J. M.; Daniels, A. D.; Kudin, K. N.; Strain, M. C.; Farkas, O.; Tomasi, J.; Barone, V.; Cossi, M.; Cammi, R.; Mennucci, B.; Pomelli, C.; Adamo, C.; Clifford, S.; Ochterski, J.; Petersson, G. A.; Ayala, P. Y.; Cui, Q.; Morokuma, K.; Malick, D. K.; Rabuck, A. D.; Raghavachari, K.; Foresman, J. B.; Cioslowski, J.; Ortiz, J. V.; Stefanov, B. B.; Liu, G.; Liashenko, A.; Piskorz, P.; Komaromi, I.; Gomperts, R.; Martin, R. L.; Fox, D. J.; Keith, T.; Al-Laham, M. A.; Peng, C. Y.; Nanayakkara, A.; Gonzalez, C.; Challacombe, M.; Gill, P. M. W.; Johnson, B.; Chen, W.; Wong, M. W.; Andres, J. L.; Gonzalez, C.; Head-Gordon, M.; Replogle, E. S.; Pople, J. A. Gaussian 98; Gaussian, Inc.: Pittsburgh PA, 1998.
15. Glendening, E. D.; Badenhoop, J. K.; Reed, A. E.; Carpenter, J. E.; Bohmann, J. A.; Morales, C. M.; Weinhold, F. NBO 5.0.; Theoretical Chemistry Institute, University of Wisconsin Madison WI 2003. Available at:http://www.chem.wisc.edu/~nbo5, accessed 16 April 2011.
16. (a) Corminboeuf, C.; Heine, T.; Weber, J. Phys Chem Chem Phys 2003, 5, 246; (b) Heine, T.; Schleyer, P. v. R.; Corminboeuf, C.; Seifert, G.; Reviakine, R.; Weber, J. J Phys Chem A 2003, 107, 6470; (c) Corminboeuf, C.; Heine, T.; Seifert, G.; Schleyer, P. v. R.; Weber, J. Phys Chem Chem Phys 2004, 6, 273.
17. (a) Biegler-König, F. W.; Schönbohm, J.; Bayles, D. J Comput Chem 2001, 22, 545; (b) Biegler-König, F. W.; Schönbohm, J. J Comput Chem 2002, 23, 1489.
18. Keith, T. A. AIMAll (Beta Version 09.08.26); 2009. Available at: http://aim.tkgristmill.com, accessed 16 April 2011

19. (a) Wang, W.-P.; Parr, R. G. Phys Rev A 1977, 16, 891; (b) Spackman, M. A.; Maslen, E. N. J Phys Chem 1986, 90, 2020; (c) Wiberg, K. B.; Bader, R. F. W.; Lau, C. D. H. J Am Chem Soc 1987, 109, 985.
20. (a) Monaco, G.; Zanasi, R.; Pelloni, S.; Lazzeretti, P. J Chem Theory Comput 2010, 6, 3343; (b) Fliegl, H.; Sundholm, D.; Taubert, S.; Jusélius, J.; Klopper, W. J Phys Chem A 2009, 113, 8668.
21. (a) Pople, J. A.; Untch, K. G. J Am Chem Soc 1966, 88, 4811; (b) Pople, J. A. J Chem Phys 1956, 24, 1111; (c) Pople, J. A. Mol Phys 1958, 1, 175.
22. Fowler, P. W.; Steiner, E. J Phys Chem A 1997, 101, 1409.
23. (a) Feixas, F.; Jiménez-Halla, J.O.C.; Matito, E.; Poater, J.; Solà, M. J Chem Theory Comput 2010, 6, 1118. (b) Feixas, F.; Matito, E.; Duran, M.; Poater, J.; Solà, M. Theor Chem Acc 2011, 128, 419.
24. Havenith, R. W. A.; Fowler, P. W. Phys Chem Chem Phys 2006, 8, 3383.
25. Bader, R. F. W. In Atoms in Molecules: A Quantum Theory; Oxford University Press: Oxford, 1990.
26. (a) Twamley, B.; Power, P. P. Angew Chem Int Ed Engl 2000, 39, 3500; (b) Kuznetsov, A. E.; Boldyrev, A. I.; Li, X.; Wang, L. -S. J Am Chem Soc 2001, 123, 8825.
27. Josélius, J.; Straka, M.; Sundholm, D.; J Phys Chem A 2001, 105, 9939.
28. Lin, Y. -C.; Juselius, J.; Sundholm, D. J Chem Phys 2005, 122, 214308.
29. (a) Mandado, M.; Krishtal, A.; Van Alsenoy, C.; Bultinck, P.; Hermida-Ramón, J. M. J Phys Chem A 2007, 111, 11885; (b) Santos, J. C.; Tiznado W.; Contreras, R.; Fuentealba P. J Chem Phys 2004, 120, 1670.
30. (a) Cossío, F. P.; Morao, I.; Jiao, H. J.; Schleyer, P. v. R. J Am Chem Soc 1999, 121, 6737; (b) Morao, I.; Lecea, B.; Cossío, F. P. J Org Chem 1997, 62, 7033.